nature structural & molecular biology

Catalysis of the microtubule on-rate is the major parameter regulating the depolymerase activity of MCAK

Jeremy R Cooper, Michael Wagenbach, Charles L Asbury & Linda Wordeman

The kinesin-13, MCAK, is a critical regulator of microtubule dynamics in eukaryotic cells. We have functionally dissected the structural features responsible for MCAK's potent microtubule depolymerization activity. MCAK's positively charged neck enhances its delivery to microtubule ends not by tethering the molecule to microtubules during diffusion, as commonly thought, but by catalyzing the association of MCAK to microtubules. On the other hand, this same positively charged neck slightly diminishes MCAK's ability to remove tubulin subunits once at the microtubule end. Conversely, dimerization reduces MCAK delivery but improves MCAK's ability to remove tubulin subunits. The reported kinetics for these events predicts a nonspecific binding mechanism that may represent a paradigm for the diffusive interaction of many microtubule-binding proteins.

The kinesin-13 protein mitotic centromere–associated kinesin (MCAK) can both rapidly depolymerize microtubules[1–3] and also provide its own means of transportation to microtubule ends, where the action of depolymerization takes place[4]. This is especially beneficial in living cells, where microtubule ends may be relatively sparse compared to microtubule lattice and are predominantly located at the cell periphery. Here, for the first time to our knowledge, we precisely quantify the relative functional benefits of two important structural features of MCAK, which are common features of microtubule motors: dimerization and the positively charged neck. We show that features that improve one function may impede another.

The MCAK neck is an α-helical ~60-amino-acid region located adjacent to the kinesin motor domain[5,6]. A high concentration of lysine and arginine residues confers a charge of about +5 on the neck at neutral pH. The positive charges in the neck are essential for MCAK to depolymerize microtubules under physiological conditions[5]. However, the mechanistic role of this structural element is entirely unknown. Hypotheses have been proposed envisioning the neck in various roles, including (i) a loose tether that allows the molecule to diffuse along the microtubule lattice[4–6], (ii) an obstructive element that prevents tight binding to the lattice[6], (iii) a 'pry bar' that destabilizes lateral interactions at the microtubule end[6] and (iv) a facilitator of cross-linking between protofilament peels at the depolymerizing ends of microtubules[7].

We used total internal reflection fluorescence (TIRF) microscopy with recombinant mammalian GFP-MCAK (from Chinese hamster, *Cricetulus griseus*) to precisely define the contribution of the positively charged neck to MCAK's microtubule depolymerization activity at the single-molecule level. We show that neither the neck nor the quaternary structure of the molecule has any significant influence on diffusion of the motor along the microtubule lattice once bound. Instead, the neck activates MCAK by increasing the flux of motors to the microtubule end. It does this by increasing the association rate of the motor to microtubules by 2 orders of magnitude. By influencing the on-rate and off-rate in parallel, the neck lowers the energy barrier for association with microtubule lattice to enable the molecules to engage in one-dimensional (1D) diffusion. In contrast, the diffusion coefficient is a relatively constant parameter for MCAK constructs that vary widely in size, structure and activity. Therefore, it is the association and dissociation rates that biological systems evolutionarily refine and functionally regulate to modulate cellular activities.

Our data show that it is the on-rate catalyzed by the neck, rather than the diffusion constant, which is similar to those of other measured microtubule diffusers, that is the single most important parameter controlling the depolymerase activity of MCAK. Unexpectedly, this important feature is used at the expense of efficacious tubulin dimer removal and underscores the compromises that arise during molecular evolution.

RESULTS

To investigate the role of MCAK's positively charged neck, we expressed and purified both full-length wild-type MCAK protein (MCAK(FL), **Fig. 1a**) and a mutant full-length MCAK protein with a neutralized neck (MCAK(FL-NN), **Fig. 1a**) in which ten of the positively charged lysine and arginine residues in the neck region were mutated to neutral alanine residues. We used a real-time microscopic assay to compare the depolymerization efficacy of enhanced green fluorescent protein–labeled MCAK(FL) (EGFP-MCAK(FL)) and EGFP-MCAK(FL-NN). Single molecules exhibited two photobleach events confirming that native single molecules of EGFP-MCAK(FL) are homodimers (**Supplementary Figure 1**). In this assay, Cy5-labeled microtubules, stabilized with the nonhydrolyzable

Department of Physiology and Biophysics, University of Washington School of Medicine, Seattle, Washington, USA. Correspondence should be addressed to L.W. (worde@u.washington.edu).

Received 20 May; accepted 22 October; published online 6 December 2009; doi:10.1038/nsmb.1728

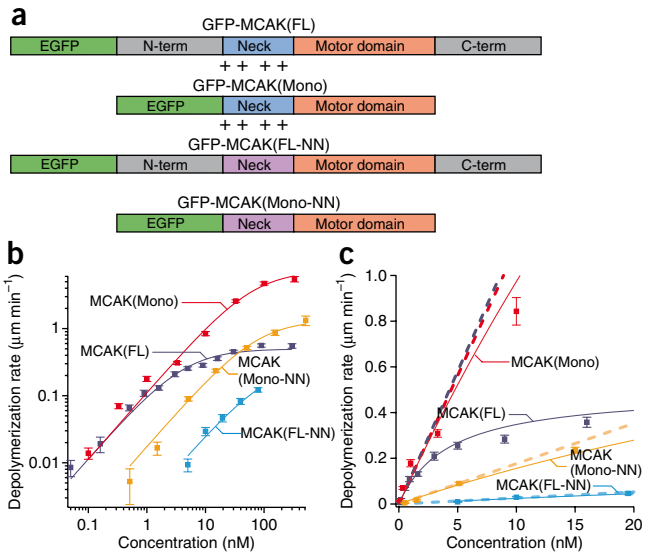

Figure 1 MCAK mutants have shifted microtubule depolymerization dose-response curves. (**a**) Diagram of mutated MCAK regions. MCAK(FL) consists of the motor domain (orange), a positively charged neck region (blue) and N- and C-terminal domains (gray). MCAK(Mono) is missing both the N- and C-terminal domains, which renders it unable to dimerize. MCAK(FL-NN) has several of the positively charged residues in the neck region replaced with neutral alanine residues (purple). MCAK(Mono-NN) combines these mutations. (**b**) Log-scale plot of average microtubule depolymerization rate versus MCAK concentration. Data from each of the four MCAK mutants is shown with a Michaelis-Menten fit curve. Error bars reflect s.e.m. values. (**c**) Linear-scale plot of the same data presented in **b**. The slope of the asymptote (dashed line) associated with each fit curve measures catalytic efficiency (k_b) (note that some of the data points at high concentration and/or depolymerization rate land off the scale of the linear plot but are included in the log-scale plot in **b**).

GTP analog GMPCPP, were tethered to a PEG-treated coverslip[8]. The ends of the microtubules were tracked over time to provide a measure of depolymerization encompassing the combined shortening rates of both microtubule ends. This was repeated over a range of MCAK concentrations to obtain a dose-response relationship (**Fig. 1b**,**c**). At low MCAK concentrations (well below saturation), we found that the dependence of the depolymerization rate on concentration approached a linear relationship (**Fig. 1c**). The catalytic efficiency, k_b, which defines this relationship, is the slope of the asymptote of a Michaelis-Menten fit to the data (**Fig. 1c**). Specifically, k_b is determined as $V_{max}/K_{1/2}$, where V_{max} and $K_{1/2}$ are the classical Michaelis-Menten parameters (**Supplementary Table 1**). The parameter k_b provides a lucid measure of the overall depolymerization efficacy as it linearly relates depolymerization rate to concentration. The mutant MCAK(FL-NN) has a k_b (0.116 μm min^{-1} nM^{-1} versus 0.0026 μm min^{-1} nM^{-1}, **Table 1**), which is lowered by a factor of 45 from that of MCAK(FL). Thus, consistent with *in vivo* data[5], neutralizing the positive charges in the neck severely cripples MCAK's ability to depolymerize microtubules.

Neck neutralization inhibits microtubule binding but not diffusion

To determine which parameters of MCAK's activity are affected by its positively charged neck, we used TIRF microscopy to image single GFP-labeled MCAK(FL) and MCAK(FL-NN) molecules as they bound to the microtubule lattice, diffused one-dimensionally along the lattice, and then dissociated. We then compared the binding kinetics and 1D diffusion of MCAK(FL) to those of MCAK(FL-NN) (**Fig. 2**). Diffusion coefficients (**Table 1**) were calculated from plots of mean square displacement versus time (**Fig. 2b**). Association and dissociation rates of binding to the microtubule lattice were calculated from the distributions of dwell times (**Fig. 2c;** see analysis section in Online Methods). Finally, using these measurements of association rate (k_{ON}), dissociation rate (k_{OFF}) and diffusion coefficient (D), we calculated the flux per concentration (J_0/C_m) of MCAK arriving at each microtubule end via lattice diffusion according to the following equation (derived from ref. 4):

$$\frac{J_0}{C_m} = \left(\frac{D}{k_{off}}\right)^{1/2} \cdot k_{on}$$

From these data (**Table 1**), we find that MCAK(FL-NN) has an enormous reduction (by a factor of 170) in lattice association rate as compared to MCAK(FL). More importantly, this difference in lattice association rate leads to a similar 140-fold reduction in MCAK(FL-NN) flux to microtubule ends. Thus, the positively charged neck is critical for MCAK delivery to microtubule ends, specifically by facilitating the initial step of binding to the microtubule lattice. The differences in diffusion coefficient and dissociation rate are much slighter (**Table 1**). These parameters, therefore, are negligible with respect to the reduced delivery of MCAK(FL-NN) to microtubule ends. These data precisely define and quantify the mechanism by which the neck domain converts the inert motor domain of MCAK into an efficient depolymerizer at physiological ionic strength.

It is also important to note that the dissociation rate of MCAK (FL-NN) is lower than that of MCAK(FL), corresponding to a longer dwell time for the neutralized-neck mutant. This unexpected finding shows that MCAK(FL-NN) molecules that are able to bind to the lattice have no trouble hanging on, clearly disproving a long-favored hypothesis that the positively charged neck acts as a tether for holding the MCAK molecule on the microtubule lattice[4–6].

Table 1 Key functional parameters of MCAK(FL) and three mutant MCAK proteins

	Catalytic efficiency (k_b) (μm min^{-1}) nM	Diffusion coefficient (D) (μm)^2 sec	Association rate (k_{ON}) (events s^{-1}) μm • nM	Dissociation rate (k_{OFF}) (events s^{-1})	Flux to microtubule end (J_0/C_m) (events s^{-1}) nM	Removal factor
MCAK(FL)	0.116 ± 0.011	0.076 ± 0.003	0.456 ± 0.008	1.70 ± 0.09	0.096 ± 0.007	18 ± 2
MCAK(FL-NN)	0.0026 ± 0.0012	0.073 ± 0.001	0.00274 ± 0.00013	1.22 ± 0.13	0.00067 ± 0.00008	58 ± 27
MCAK(Mono)	0.112 ± 0.013	0.090 ± 0.003	6.99 ± 0.09	3.98 ± 0.13	1.05 ± 0.05	1.6 ± 0.2
MCAK(Mono-NN)	0.018 ± 0.003	0.051 ± 0.002	0.323 ± 0.015	1.58 ± 0.11	0.058 ± 0.005	4.5 ± 0.9

The catalytic efficiency (k_b) is calculated from a Michaelis-Menten fit to the depolymerization-rate dose-response data (**Fig. 1**). Diffusion coefficients (D) were measured from a plot of mean square displacement versus time (**Fig. 2b**) and reflect only the diffusion parallel to the axis of the microtubule (the perpendicular component is very close to zero). Association rates (k_{ON}) and dissociation rates (k_{OFF}) were calculated from the dwell-time distributions of landing events (**Fig. 2c**). The flux of MCAK molecules arriving at each microtubule end via lattice diffusion (J_0/C_m) was calculated from D, k_{ON} and k_{OFF} using the flux equation noted in the text. The removal factor is an estimate of the number of tubulin subunits removed on average for a single MCAK end-binding event (see Online Methods).

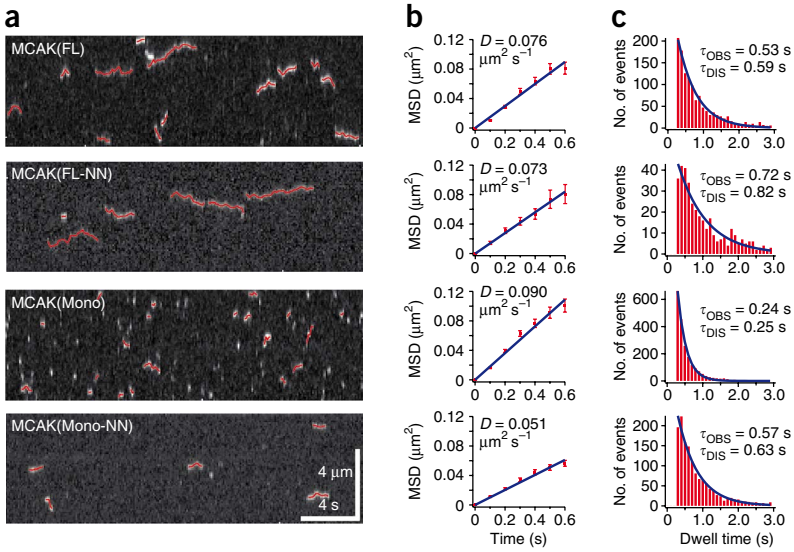

Figure 2 Diffusive behavior of single MCAK molecules and mutants. (**a**) Kymographs demonstrate single-molecule diffusion of MCAK(FL) and mutant MCAK proteins. All four of the tested MCAK proteins can bind to and diffuse along the microtubule lattice, although with radically different association rates (k_{ON}) and dissociation rates (k_{OFF}). Two-dimensional Gaussian-fit tracks of the moving spots are overlaid in red. (**b**) The mean square displacements for each of the four tested MCAK proteins are shown plotted at 0.1-s intervals. Diffusion coefficients (D) are calculated as half the slope of the fit line. (**c**) Distributions of event dwell times for each of the four tested MCAK proteins shown with a single exponential fit curve. τ_{OBS} reflects the observed average event duration. τ_{DIS} has been corrected for photobleaching and is thus the average time before event dissociation.

Neck neutralization facilitates tubulin removal

We then asked whether the positively charged neck might aid in MCAK's ability to depolymerize microtubules after arrival at the microtubule end, as previously proposed[6,7]. To answer this question, we calculated the average number of tubulin subunits that are removed for each MCAK end-binding event (which we refer to as the "removal factor") for both MCAK(FL) and MCAK(FL-NN). The removal factor is calculated by dividing k_b (with units converted to express the depolymerization rate as the number of tubulin subunits removed from each microtubule end per second; see analysis in Online Methods) by J_0/C_m. Unexpectedly, we found that MCAK(FL-NN) on average removes more than three times as many tubulin subunits per end-binding event than MCAK(FL) (58 versus 18 tubulin subunits removed, **Table 1**). This indicates that the positively charged neck substantially impedes MCAK's ability to remove tubulin subunits from the microtubule end. If the removal factor is an indirect measure of processivity, then we speculate that the reduced dissociation rate enhances the processivity of MCAK motors. This would be the first demonstration to our knowledge that removing positive charges on the neck domain enhances processivity and represents a mechanistic specialization of depolymerizing kinesins. For motile kinesins, the addition of positive charges generally leads to an increase in processivity[9]. Despite the detrimental effect of reduced processivity, the benefit that the positively charged neck provides in terms of delivery of MCAK to the microtubule end affords MCAK(FL) a general advantage over MCAK(FL-NN) as quantified by k_b. Thus, the benefit of the positively charged neck, with regard to increasing the association rate of MCAK to microtubules, outweighs the disadvantage it imparts in slightly impeding the removal of tubulin subunits.

Dimerization inhibits microtubule binding

We similarly characterized the contribution of MCAK's native homodimeric quaternary structure. MCAK's ability to dimerize depends on both its N- and C-terminal domains[10]. The specific role of dimerization is not well understood owing to the fact that monomeric mutants containing only the neck and motor (and lacking the N- and C-terminal dimerization domains) depolymerize quite well[5,10,11]. A recent study suggests that monomeric MCAK (MCAK(Mono)) may have a more difficult time disengaging from detached tubulin subunits than does full-length dimeric MCAK[12]. Thus, dimerization has been hypothesized to improve MCAK's functionality by promoting the release of the enzyme from detached tubulin subunits so that it can to undergo multiple rounds of action. However, overexpressed MCAK(Mono) generally outperforms MCAK(FL) as a microtubule depolymerizer in cells[5,10,11]. This apparent contradiction led us to perform a thorough analysis of the role of dimerization in the absence of free tubulin in order to eliminate any effect of tubulin sequestration. This enabled us to specifically determine the effect that dimerization has on MCAK's two most important activities with respect to the microtubule: transport to microtubule ends and tubulin subunit removal.

We expressed and purified GFP-labeled MCAK(Mono) (**Fig. 1a**) in which the N- and C-terminal dimerization domains had been deleted but the neck and motor domain were retained, as in previously described monomeric mutants[10]. We determined k_b, association rate, dissociation rate, diffusion coefficient, flux to microtubule end, and removal factor for MCAK(Mono). Unexpectedly, the monomeric mutant MCAK(Mono) has a 15-fold higher association rate with the microtubule lattice than MCAK(FL) (**Table 1**). In addition, MCAK(Mono) has a twofold higher dissociation rate (corresponding to shorter dwell times on the microtubule lattice) and a 20% higher diffusion coefficient. However, the association rate provides the dominant influence, resulting in a net 11-fold higher flux to microtubule ends for MCAK(Mono). Thus, dimerization inhibits the delivery of MCAK to microtubule ends, primarily as a result of reduced lattice association rates.

Dimerization facilitates tubulin removal

The removal factor for MCAK(Mono) is lower by a factor of 11 (**Table 1**) than that of the MCAK(FL). Thus, once the MCAK molecule arrives at the microtubule end, dimerization greatly enhances its ability to remove tubulin subunits. It might appear that in the case of dimerization, the benefits and detriments balance each other out, as the overall depolymerization efficacy as quantified by k_b reveals a nearly equal performance between MCAK(Mono) and MCAK(FL). However, for situations in which the delivery of MCAK to microtubule ends is enhanced by means other than lattice diffusion (such as recruitment by end-binding protein 1 (EB1) (ref. 13) or direct anchoring to centromeres during mitosis), we would expect MCAK(FL) to depolymerize more effectively than MCAK(Mono). The reported enhanced ability of MCAK(FL) to disengage from detached tubulin subunits[12] might further improve the effectiveness of the full-length enzyme in cells. Finally, the C terminus of MCAK limits the tendency of the enzyme to hydrolyze ATP unproductively along the lattice[14]. In this way, the coupling of ATP hydrolysis to tubulin removal might be

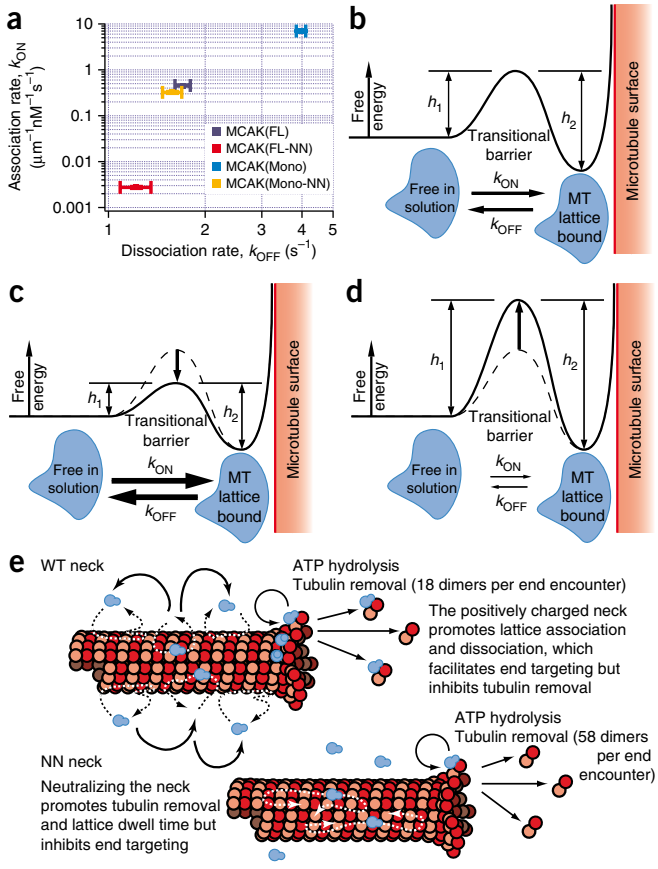

Figure 3 A positive correlation between k_{ON} and k_{OFF} is consistent with an energy-landscape model for diffusive binding. (**a**) Association rates (k_{ON}) for MCAK(FL) and each of the three tested MCAK mutants plotted against the respective dissociation rates (k_{OFF}). This plot demonstrates a positive relationship between k_{ON} and k_{OFF}, which can be explained by a transitional barrier of variable height as shown in **b**. The MCAK molecule (blue) must pass through the high-energy transitional state in order to switch between the two stable low-energy states, free in solution or microtubule bound. k_{ON} represents the transition from free-in-solution to the microtubule-bound state and is inversely dependent upon the height h_1. Alternately, k_{OFF} represents the transition from microtubule-bound to free-in-solution state and is inversely dependent on the height h_2. (**c**) The data indicates that MCAK(Mono) has a reduced barrier height in comparison to MCAK(FL), which explains the observed increases in both k_{ON} and k_{OFF}. (**d**) Conversely, MCAK(FL-NN) has an increased barrier height, indicated by the observed decreases in both k_{ON} and k_{OFF}. (**e**) Model illustrating the parameters that affect the flux of motors to the microtubule end and the removal of tubulin from the microtubule end.

improved by domains outside the core neck and motor at the expense of a slightly reduced lattice association rate[12,14].

In contrast to the comparable performance observed between MCAK(Mono) and MCAK(FL) at low concentrations, MCAK(Mono) substantially outperforms MCAK(FL) at saturating concentrations as quantified by a 15-fold higher V_{max}. This observation explains prior studies that showed MCAK(Mono) outperforming MCAK(FL) when each were overexpressed in cells[5,10,11]. The cells in these assays almost certainly encounter saturating concentrations of MCAK; thus, the data presented here would predict that MCAK(Mono) should show more effective depolymerization.

To verify the findings regarding the specific functionality of MCAK's positively charged neck and dimerization, we expressed and purified a mutant comprising a combination of the previous two mutations (MCAK(Mono-NN), **Fig. 1a**). We measured k_b, association rate, dissociation rate, diffusion coefficient, flux to microtubule end, and removal factor for this mutant. As verification of the function of the positively charged neck, we expected to see the same trends when comparing MCAK(Mono-NN) to MCAK(Mono) as we observed when comparing MCAK(FL-NN) to MCAK(FL), namely a lower lattice association rate, a lower flux to the microtubule end, and a greater removal factor. As predicted, MCAK(Mono-NN) has a lower lattice association rate (roughly by a factor of 22), and a lower (by a factor of 18) flux to the microtubule end, but a higher removal factor (by a factor of 3) than MCAK(Mono). Likewise, as verification of the function of dimerization, we expected a comparison between MCAK(Mono-NN) and MCAK(FL-NN) to yield similar trends as we observed between MCAK(Mono) and MCAK(FL): a higher lattice association rate, a higher flux to the microtubule end, and a lower removal factor. The data matched these expectations, with MCAK(Mono-NN) showing a higher lattice association rate (by a factor of 120), a higher flux to the microtubule end (by a factor of 90), and a lower (by a factor of 13) removal factor than MCAK(FL-NN).

MCAK is likely to be processive but not cooperative

In addition to explaining functional contributions of MCAK's positively charged neck and dimeric structure, these data also provide several additional insights into the mechanism of MCAK operation. First, in addition to the Michaelis-Menten fit to the dose-response depolymerization data (**Fig. 1b**), we also fit the Hill equation to this data as a means to determine whether MCAK shows cooperativity (**Supplementary Fig. 2**). The Hill fit yields n values very close to 1 for MCAK(FL) and each of the three mutants (**Supplementary Fig. 2**). This suggests that MCAK molecules do not act cooperatively, but rather as individual depolymerizing enzymes.

Second, as suggested above, the removal-factor data (**Table 1**) are consistent with MCAK acting processively (undergoing multiple enzymatic cycles of tubulin subunit removal) at the microtubule end. Furthermore, neutralization of the neck, while decreasing the on-rate and flux to the microtubule end, may increase the processivity of the motor once it reaches the end. However, because the binding of one MCAK molecule at the microtubule end might have a net destabilization effect resulting in the simultaneous removal of several tubulin subunits, future single-molecule analysis focused specifically on the action of MCAK molecules at the ends of microtubules will be required to establish whether or not MCAK acts processively.

An energy barrier must be negotiated to bind microtubule lattice

Plotting the microtubule lattice association rate versus dissociation rate for each of the four mutants unexpectedly revealed a positive trend (**Fig. 3a**). Stated explicitly, a mutant such as MCAK(Mono) associates with the microtubule lattice more frequently than MCAK(FL) but is also more quick to fall off. Conversely, MCAK (FL-NN) very infrequently initiates an interaction with the microtubule lattice, but once it does, it is more likely to remain attached than wild-type MCAK(FL) or any of the other mutants. In terms of the energy landscape, this implies that there is a barrier between the free-in-solution state and the lattice-bound state that can be raised or lowered with certain mutations to the molecule (**Fig. 3b**). A mutant such as MCAK(Mono) has a low barrier and is therefore able to transition in either direction between the free-in-solution and lattice-bound states with high frequency (**Fig. 3c**). By contrast, MCAK(FL-NN) has a high barrier, and thus its transitions between the two states occur relatively infrequently (**Fig. 3d**).

DISCUSSION

Our data show that the function of the positively charged neck of MCAK is to negotiate an energy barrier that naturally impedes the direct association of the motor (and likely most microtubule-associated proteins) with the microtubule lattice. The barrier also impedes dissociation from the microtubule once the protein is bound. Crossing the barrier is so important that a reduction in tubulin-removal efficiency is tolerated to catalyze it. The source of this barrier represents a fundamental question for future experiments in this area. One possible mechanism for generating such a barrier is a transitional restructuring of the hydration shell and associated ions that surround the MCAK molecule and the microtubule lattice. This type of water-shell remodeling has been shown to occur in the nonspecific association of DNA-binding proteins into the major and minor grooves of DNA[15]. DNA has a negatively charged surface, which polarizes and imparts additional structure to the water molecules in its immediate vicinity[16]. The arrival of a binding protein within this space remodels these hydration shells, which requires a high free energy during the transition[17]. Like DNA, microtubules carry a strong negative charge along their surface, and thus we would expect to observe an analogous phenomenon. The potential significance of such a transitional state is that the high free energy required to cross the transitional barrier could serve to maintain attachment of the binding protein without the need for a strong binding motif. This would allow the binding protein, MCAK in this case, to diffuse somewhat freely along the microtubule yet not fall off, in a process similar to the rapid 1D diffusion observed with DNA binding proteins. Furthermore, it offers a common mechanism to explain the ever-growing number of diverse proteins that have been shown to undergo 1D diffusion along microtubules, including MCAK[4], the Dam1 complex[8], Eg5 (ref. 18), myosin V[19], CENP-E[20] and the Ndc80 complex[21].

The highly nonspecific and loose interaction of MCAK diffusing on microtubules is maintained not by direct binding groups but instead by entropic restructuring of the surrounding water and ions. Our study contradicts the idea that 1D diffusion of motors like MCAK is a modified version of directed motility (randomly directed stepping[22]). Many nonmotor molecules diffuse similarly on microtubules, and MCAK does not 'step' like a motile kinesin[4,23]. Providing further support for this conclusion is our observation that the motor domain of MCAK is not necessary for diffusion because purified motorless MCAK diffuses avidly and with a similar diffusion coefficient to that of wild-type motor (data not shown). This study also contradicts that idea that diffusive behavior is conferred by a specific 'diffusion domain'. The positively charged neck domain of MCAK has been previously implicated as a domain that could electrostatically tether MCAK to microtubules during diffusion[3,4]. We have shown, by removing the electrostatic charges in the neck without adversely affecting diffusion, that this is not the case.

The positively charged neck domain of MCAK is, however, an absolute requirement for the protein to have microtubule depolymerization activity under physiological conditions[5]. In contrast to being a tether for diffusion, the neck catalyzes the association of motor to microtubules. The association constant for MCAK(FL) to microtubule ends is 96 μM^{-1} s^{-1}, which is substantially higher than the typical range of on-rates for 3D diffusion–limited protein associations (0.5–8 μM^{-1} s^{-1}) (ref. 24). Tubulin and actin polymerization, for example, fall within this latter range[25,26]. The rate at which MCAK could find the microtubule end, 96 μM^{-1} s^{-1}, is within 2 orders of magnitude of the maximum theoretical association value of 7,000 μM^{-1} s^{-1} predicted by the Einstein-Smoluchowski equation[27] for a situation without geometric constraints. Few association reactions approach this maximum rate (and most fall many orders of magnitude short) even with facilitated diffusion afforded by either coulombic forces or reduction in dimensionality. We have parsed apart the relative contributions of these mechanisms by showing that the on-rate for MCAK(FL-NN) to microtubule ends (0.67 μM^{-1} s^{-1}) is ~1/150 of the on-rate for MCAK(FL). Thus, the positively charged neck increases the on-rate to microtubule ends approximately 150-fold. This can be compared to the contribution of the reduction in dimensionality by diffusion, or the "antenna effect"[4]. In this case, the on-rates of MCAK(FL) and MCAK(FL-NN) to the microtubule lattice are 3.6 μM^{-1} s^{-1} and 0.022 μM^{-1} s^{-1}, respectively, whereas the on-rates to microtubule ends are, as stated above, 96 μM^{-1} s^{-1} and 0.67 μM^{-1} s^{-1}, respectively. In both cases, diffusion along the lattice increases the on-rate to microtubule ends in MCAK(FL) and MCAK(FL-NN) by about 30-fold. This substantial enhancement of microtubule depolymerizing activity over the 3D diffusion–limited on-rate has been demonstrated previously[4]. But we show here that 1D diffusion is a constant for both MCAK(FL) and highly inefficient MCAK mutants. Collectively, then, the high on-rate of MCAK to microtubule ends is facilitated by a combination of on-rate catalysis by a factor of 150) and reduction in dimensionality (by a factor of 30). Most importantly, we have shown that it is the on-rate, not the diffusion coefficient, that varies among mutant MCAK variants. This suggests that tuning the on-rate is the way that cells control microtubule depolymerase activity over an extremely broad kinetic range and is likely a major driving force during molecular evolution.

It is interesting that either the addition of positive charges to the neck or the removal of dimerization domains increases both the association and the dissociation of MCAK with the microtubule lattice in parallel. A modest increase in the dissociation rate in parallel with the on-rate may be tolerated to traverse the energy barrier surrounding the microtubule. This property may instead help to drive the delivery of MCAK to microtubule ends by enabling the molecule to hop from one diffusive site to another (**Fig. 3e**), as with MCAK(Mono). Without this capability, the motor may tend to scan the same region on the microtubule repeatedly, resulting in a decrease in the flux of motor to the microtubule end.

The performance enhancement imparted by the positively charged neck comes with a tradeoff, in that the protein's effectiveness at removing tubulin subunits is reduced. Conversely, dimerization affords MCAK an improved ability to remove tubulin subunits once at the microtubule end, but this improvement is countered by a reduction in microtubule lattice association rate. Some of the reduced performance in lattice binding could potentially be offset *in vivo* by direct recruitment of MCAK to microtubule ends at centromeres or by EB1 (ref. 13). Regardless, catalysis of the association of MCAK with microtubules is the most important parameter controlling the efficiency of MCAK's depolymerizing activity. The structures that catalyze microtubule association constitute superb candidate domains for cellular regulation of MCAK and most likely that of any protein that diffuses on microtubules.

METHODS

Methods and any associated references are available in the online version of the paper at http://www.nature.com/nsmb/.

Note: Supplementary information is available on the Nature Structural & Molecular Biology website.

ACKNOWLEDGMENTS

The authors acknowledge support from the National Institutes of Health (GM069429) and from the National Science Foundation (IGERT traineeship to J.C.).

AUTHOR CONTRIBUTIONS
J.R.C. built the TIRF microscope, developed the coverslip coating and assay conditions, purified some of the protein samples, wrote the analysis software, performed all of the experiments and wrote the manuscript. M.W. engineered the DNA constructs and purified and calibrated some of the protein samples. C.L.A. assisted with the TIRF configuration. L.W. oversaw the entire project, suggested experiments and assisted with data interpretation and also with the writing of the manuscript.

Published online at http://www.nature.com/nsmb/.
Reprints and permissions information is available online at http://npg.nature.com/reprintsandpermissions/.

1. Wordeman, L., Wagenbach, M. & von Dassow, G. MCAK facilitates chromosome movement by promoting kinetochore microtubule turnover. *J. Cell Biol.* **179**, 869–879 (2007).
2. Desai, A., Verma, S., Mitchison, T.J. & Walczak, C.E. Kin I kinesins are microtubule-destabilizing enzymes. *Cell* **96**, 69–78 (1999).
3. Hunter, A.W. *et al.* The kinesin-related protein MCAK is a microtubule depolymerase that forms an ATP-hydrolyzing complex at microtubule ends. *Mol. Cell* **11**, 445–457 (2003).
4. Helenius, J., Brouhard, G., Kalaidzidis, Y., Diez, S. & Howard, J. The depolymerizing kinesin MCAK uses lattice diffusion to rapidly target microtubule ends. *Nature* **441**, 115–119 (2006).
5. Ovechkina, Y., Wagenbach, M. & Wordeman, L. K-loop insertion restores microtubule depolymerizing activity of a "neckless" MCAK mutant. *J. Cell Biol.* **159**, 557–562 (2002).
6. Ogawa, T., Nitta, R., Okada, Y. & Hirokawa, N. A common mechanism for microtubule destabilizers-M type kinesins stabilize curling of the protofilament using the class-specific neck and loops. *Cell* **116**, 591–602 (2004).
7. Moores, C.A. *et al.* The role of the kinesin-13 neck in microtubule depolymerization. *Cell Cycle* **5**, 1812–1815 (2006).
8. Gestaut, D.R. *et al.* Phosphoregulation and depolymerization-driven movement of the Dam1 complex do not require ring formation. *Nat. Cell Biol.* **10**, 407–414 (2008).
9. Thorn, K.S., Ubersax, J.A. & Vale, R.D. Engineering the processive run length of the kinesin motor. *J. Cell Biol.* **151**, 1093–1100 (2000).
10. Maney, T., Wagenbach, M. & Wordeman, L. Molecular dissection of the microtubule depolymerizing activity of mitotic centromere-associated kinesin. *J. Biol. Chem.* **276**, 34753–34758 (2001).
11. Newton, C.N., Wagenbach, M., Ovechkina, Y., Wordeman, L. & Wilson, L. MCAK, a Kin I kinesin, increases the catastrophe frequency of steady-state HeLa cell microtubules in an ATP-dependent manner in vitro. *FEBS Lett.* **572**, 80–84 (2004).
12. Hertzer, K.M. *et al.* Full-length dimeric MCAK is a more efficient microtubule depolymerase than minimal domain monomeric MCAK. *Mol. Biol. Cell* **17**, 700–710 (2006).
13. Honnappa, S. *et al.* An EBI-binding motif acts as a microtubule tip localization signal. *Cell* **138**, 366–376 (2009).
14. Moore, A. & Wordeman, L. C-terminus of mitotic centromere-associated kinesin (MCAK) inhibits its lattice-stimulated ATPase activity. *Biochem. J.* **383**, 227–235 (2004).
15. Privalov, P.L. *et al.* What drives proteins into the major or minor grooves of DNA? *J. Mol. Biol.* **365**, 1–9 (2007).
16. Kopka, M.L., Fratini, A.V., Drew, H.R. & Dickerson, R.E. Ordered water structure around a B-DNA dodecamer. A quantitative study. *J. Mol. Biol.* **163**, 129–146 (1983).
17. Levy, Y. & Onuchic, J.N. Water mediation in protein folding and molecular recognition. *Annu. Rev. Biophys. Biomol. Struct.* **35**, 389–415 (2006).
18. Kapitein, L.C. *et al.* The bipolar mitotic kinesin Eg5 moves on both microtubules that it crosslinks. *Nature* **435**, 114–118 (2005).
19. Ali, M.Y. *et al.* Myosin Va maneuvers through actin intersections and diffuses along microtubules. *Proc. Natl. Acad. Sci. USA* **104**, 4332–4336 (2007).
20. Kim, Y., Heuser, J.E., Waterman, C.M. & Cleveland, D.W. CENP-E combines a slow, processive motor and a flexible coiled coil to produce an essential motile kinetochore tether. *J. Cell Biol.* **181**, 411–419 (2008).
21. Powers, A.F. *et al.* The Ndc80 kinetochore complex uses biased diffusion to couple chromosomes to dynamic microtubule tips. *Cell* **136**, 865–875 (2009).
22. Bormuth, V. *et al.* Protein friction limits diffusive and directed movements of kinesin motors on microtubules. *Science* **325**, 870–873 (2009).
23. Cooper, J.R. & Wordeman, L. The diffusive interaction of microtubule binding proteins. *Curr. Opin. Cell Biol.* **21**, 68–73 (2009).
24. Northrup, S.H. & Erickson, H.P. Kinetics of protein-protein association explained by Brownian dynamics computer simulation. *Proc. Natl. Acad. Sci. USA* **89**, 3338–3342 (1992).
25. Pollard, T.D. & Cooper, J.A. Actin and actin-binding proteins. A critical evaluation of mechanisms and functions. *Annu. Rev. Biochem.* **55**, 987–1035 (1986).
26. Caplow, M. *et al.* The free energy for hydrolysis of a microtubule-bound nucleotide triphosphate is near zero: all of the free energy for hydrolysis is stored in the microtubule lattice. *J. Cell Biol.* **127**, 779–788 (1994).
27. Smoluchowski, S. Versuch einer mathematischen Theorie der koagulationskinetik kolloider Losungen. *Z. Phys. Chem.* **92**, 129–168 (1918).

ONLINE METHODS

Protein expression. We purified wild-type and mutant EGFP-labeled MCAK proteins as described[10], except that the pFastBac1 plasmid (Invitrogen) was used to construct recombinant baculoviruses. MCAK(FL-NN) includes point mutations that introduce positively charged amino acid residues in the neck as described[5] (see **Fig. 1** for diagrams of the MCAK mutants). Concentrations of monomeric mutants (MCAK(Mono) and MCAK(Mono-NN)) are reported as concentrations of active ATP-binding sites. For dimeric mutants (MCAK(FL) and MCAK(FL-NN)), the concentration of active ATP-binding sites was divided by 2 to provide a true molecular concentration.

Microtubules. We purified tubulin from bovine brains and fluorescently labeled tubulin with Cy5 *N*-hydroxysuccinimide ester dye (Amersham) per standard techniques[28,29]. Guanalyl-(α,β)-methylene diphosphate (GMPCPP)-stabilized microtubules were grown at 37 °C from a 30:1 mixture of unlabeled and Cy5-labeled tubulin. Taxol-stabilized microtubules were grown at 37 °C from a 300:1 mixture of unlabeled and Cy5-labeled tubulin in BRB80 (80 mM PIPES, pH 6.8, 1 mM $MgCl_2$, 1 mM EGTA) + 5% DMSO, 5 mM $MgCl_2$ and 2 mM GTP and immediately diluted into BRB80 + 10 μM taxol (Sigma). Microtubules were pelleted to remove unpolymerized tubulin and then resuspended in BRB80 + 10 μM taxol.

TIRF configuration. We collected TIRF data using a Nikon TE2000-S inverted microscope with a custom two-color TIRF illumination system. The TIRF configuration was objective based using a 100×, 1.49–numerical aperture (NA) Nikon objective. GFP was excited with a 473-nm laser (LaserPath Technologies) and Cy5 with a 637-nm laser (Blue Sky Research). We recorded simultaneous red and green images on an Andor Ixon DV887ECS-BV back-illuminated electron-multiplying charge-coupled device (EMCCD).

Depolymerization assay conditions. After initially rinsing with distilled, deionized H_2O, we filled flow chambers constructed with double-sided tape with BRB80 + 70 mM KCl, 1 mg ml^{-1} κ-casein (Sigma) and ~10 μg ml^{-1} G234A rigor-kinesin[30]. After incubation for ~5 min, flow chambers were rinsed thoroughly with BRB80 + 70 mM KCl and 1 mg ml^{-1} κ-casein.

For depolymerization assays, GMPCPP-stabilized microtubules were drawn into the chamber and allowed to link up to the surface-bound rigor-kinesin. After incubation for ~5 min, the chamber was rinsed and assay buffer containing MCAK(FL) (or one of the three mutant forms) was drawn into the chamber. Assay buffer was composed of BRB80 + 70 mM KCl, 1 mg ml^{-1} κ-casein, 2 mM ATP, 200 μg ml^{-1} glucose oxidase, 35 μg ml^{-1} catalase, 25 mM glucose and 5 mM DTT. Images were recorded at 1 frame per second.

For single-molecule assays, the flow chambers were prepared in the same manner as for depolymerization assays (described above), except taxol-stabilized microtubules were used and images were recorded at 10 frames per second.

Photobleach measurements. For single-molecule photobleach measurements, the flow chambers were prepared identically except that nucleotides were omitted, resulting in MCAK molecules binding the microtubule lattice in a rigor-like fashion such that the photobleach rates could be measured without dissociation of the molecule (**Supplementary Fig. 1** provides four examples of the characteristic two-step photobleach pattern observed for dimeric EGFP-labeled MCAK(FL)). The average photobleach rate for EGFP under the conditions of the single-molecule experiments was measured using MCAK(Mono), which, being a monomer, undergoes one-step photobleach events. This rate was used to correct the measurement of the average dwell time for photobleaching effects (see below).

Analysis. Movies were imported into Igor Pro 6.0 (Wavemetrics) for analysis. Custom routines written within the Igor programming environment were used to analyze both depolymerization rates and single-molecule kinetics. An edge-finder routine was applied to the microtubule kymographs at each time point to calculate the instantaneous length of the microtubule throughout the movie. The depolymerization rate for each microtubule was measured by fitting a regression line to the length-versus-time curve; thus, this measurement reflects the combined depolymerization of both microtubule ends. Each data point shown in the dose-response curve (**Fig. 1**) represents an average of between 20 and 50 microtubules imaged from at least two but usually three or more separate flow cells. An average baseline depolymerization rate of 0.005 μm min^{-1} was calculated from microtubules from five separate flow cells, prepared as described above but lacking MCAK. This baseline rate was subtracted from each of the individual depolymerization rate measurements to obtain the final dose-response data. Data were fit to both the Michaelis-Menten equation (**Fig. 1**) to yield the parameters V_{max} and $K_{1/2}$ and the Hill equation (**Supplementary Fig. 2**) to yield the parameters V_{max}, $K_{1/2}$, and n.

Single-molecule landing events were tracked by fitting a 2D Gaussian function frame by frame to every bright spot that landed on the microtubule lattice and dwelled there for 0.3 s (three frames) or longer. Displacements were measured longitudinally to the microtubule axis, and mean square displacements were calculated at 0.1-s increments. Diffusion coefficients were calculated as described[4]. The fact that the diffusion coefficient measured here is lower that that from a previously published study of MCAK[4] is most likely due to the differences in the source of tubulin (species and post-translational modifications) for the microtubules used in the assays and to differences in the ionic strengths of the solutions between the two studies. The diffusion coefficients measured in this study are fully consistent with others measured using the same microtubules[8]. Dissociation rates were calculated by fitting a single exponential to each histogram of dwell times (**Fig. 2**) and taking the reciprocal of the time constant, τ_{DIS}. This measurement was corrected for the effects of photobleaching as described[4]. The total number of events was estimated by integrating the exponential fit to the dwell-time histogram from 0 to ∞. This is more accurate than simply counting up events because it accounts for the 'missing events' that have a shorter dwell time than the threshold of 0.3 s. The calculation of the total number of events was then divided by the total time, microtubule length, and concentration to achieve a measurement of the association rate onto the microtubule lattice. These measured kinetic parameters were averaged from thousands of events from at least four separate flow cells (per mutant) imaged on different days.

The removal factor was calculated by first converting the catalytic efficiency (k_b) to a measure of tubulin subunits removed from each microtubule end per second per nanomole. A conversion factor of 1,750 tubulin subunits per micron of microtubule length was used and the result was subsequently divided by 2 to account for the fact that depolymerization rates were a measure of the combined shortening rates of both microtubule ends. Finally, this number was divided by the flux of MCAK to each microtubule end (J_0/C_m) to yield a measure of the average number of tubulin subunits removed for each MCAK end-binding event.

28. Hyman, A. *et al.* Preparation of modified tubulins. *Methods Enzymol.* **196**, 478–485 (1991).
29. Mickey, B. & Howard, J. Rigidity of microtubules is increased by stabilizing agents. *J. Cell Biol.* **130**, 909–917 (1995).
30. Rice, S. *et al.* A structural change in the kinesin motor protein that drives motility. *Nature* **402**, 778–784 (1999).